Numerical Methods in Civil Engineering, 7-2 (2022) 33-41

Numerical Methods in Civil Engineering

Journal Homepage: https://nmce.kntu.ac.ir/

Numerical investigation of the effects of geotechnical parameters on building risk level due to mechanized tunneling in urban areas

Mohammad Ali Iranmanesh* **and Ali Arianfar****

ARTICLE INFO

RESEARCH PAPER

Article history:
Received:
April 2022.
Revised:
June 2022.
Accepted:
June 2022.

Keywords:
Mechanized tunneling,
Surface settlement,
Risk level of building,
Numerical simulation,
Vulnerability index

Abstract:

In this study, the effects of some geotechnical parameters on the surface settlement curves due to mechanized tunneling and the corresponding risk on surface buildings are investigated through numerical analysis. The advanced constitutive law of Plastic Hardening is utilized to accurately reflect the Soil behavior in unloading. Using the surface settlement curves obtained from numerical analysis, the risk category of surface buildings are calculated and the effectiveness of each parameter on the risk level is investigated. The results show that the cohesion and friction angle do not have a remarkable effect on surface settlement and the corresponding risk. However, the amount of overburden and the soil elastic modulus considerably affect the surface settlement and the risk level subjected to the surface buildings. Recognizing the role of each parameter makes it possible to predict the potential risk on surface buildings and to optimize the approaches for mitigating these risks.

1. Introduction

Urban excavation near existing structures changes the stress distribution within the soil and thus, exposes the structures to unwanted risks and inevitable displacement beneath the structures. Different mechanical and physical parameters of soil, overburden, foundation depth and the horizontal distance between the tunnel axis and the building, as well as building type and its vulnerability, affect the risk imposed on the building due to excavation. Determining the effects and the level of risk for buildings above the tunnel can enable the experts to consider proper measures and prevent potential severe damages.

Estimation of surface settlement is one of the critical principles of designing an urban tunnel that should be carried out accurately and correctly to prevent damage to the surface and non-surface structures. Generally, tunnel excavation in any depth changes the stress distribution and convergence pattern around tunnel opening, resulting in the surface settlement [1].

* *Corresponding author: Assistance Professor, Faculty of Civil Engineering, K. N. Toosi University of Technology, Tehran, Iran. Email: iranmanesh@kntu.ac.ir*

** *Ph.D. Graduate, Faculty of Mining, Petroleum & Geophysics Engineering, Shahrood University of Technology, Semnan, Iran.*

The degree and type of settlement rely on factors including geological and geotechnical conditions (e.g., mechanical properties of soil and groundwater), depth and geometry of the tunnel, and how the tunnel is constructed [2,3]. Figure 1 shows a three-dimensional view of ground settlement due to tunnel excavation.

Analytic methods for the surface settlement due to tunnel excavation are essentially based on previous experiences, and face many limitations [4]. Analytic methods in which the geotechnical properties of the ground are not accounted for cannot provide an efficient solution. Considering the software and hardware advancements, the use of numerical methods based on actual geotechnical parameters and constitutive models consistent with expected behavior is a reasonable solution for the accurate determination of surface settlement curve due to excavation. A relatively large body of literature has addressed the ground settlement due to tunnel excavation [5-11]. In recent years, several methods have been proposed to calculate the settlement due to tunnel excavation which analytic-empirical and numerical methods are the most important ones. Empirical methods that are based on empirical expressions, derived from previous

observations which use previous experiences to determine parameters such as volume loss [4,12]. They also account for tunneling methods and ground conditions in terms of some parameters.

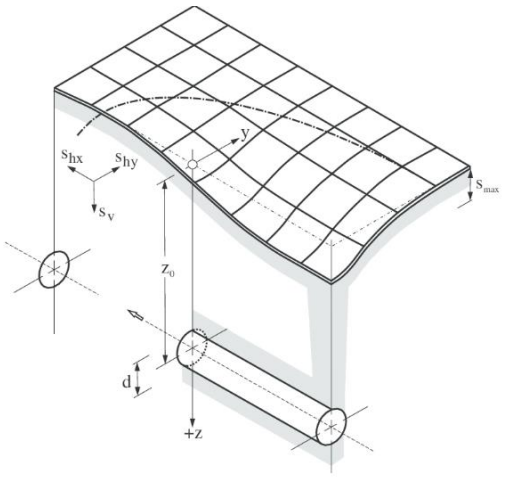

Fig. 1: Three-dimensional ground settlement due to tunnel excavation.

Numerical methods are a suitable and flexible tool to estimate surface settlement for 2D and 3D problems. However, they are challenging to adopt, and they need special consideration due to the complexity and sensitivity of these methods to soil, structure, and construction procedure parameters. In general, computational technology advancements have turned numerical methods into a robust tool for settlement estimation [13-15, 17-20].

Tunnel overburden, modulus of elasticity, cohesion, and angle of internal friction were considered to determine the effect of geotechnical parameters on the surface settlement curve and the risk level of surface structure. Then, a particular value was assigned to each parameter as the baseline, and for each model, only one of the parameters was considered a variable. Thus, using FLAC finite difference software, nine models were evaluated to derive the surface settlement curve. Plastic hardening was chosen as the constitutive law for numerical modeling. The surface settlement expressions which derived for all nine cases were used to determine the risk category of a 5-story ten m-wide building with a foundation depth of 3 m and various vulnerabilities (five different categories of vulnerability), located at different horizontal distances to the tunnel axis. Finally, the identified risk categories were used to assess the effect of study parameters on the level of risk.

2. Formulation

Peck (1969) presented the first comprehensive study of empirical methods. In fact, Peck's paper has been the foundation of all subsequent studies regarding the settlement of soft soils due to tunnel excavation [16]. He showed that the cross-section of the settled zone due to tunneling is a Gaussian distribution function that shows the vertical displacement of the ground surface as follows:

$$S_v = S_{v,\max} \exp\left(\frac{-x^2}{2i^2}\right) \quad (1)$$

Where S_v denotes the vertical displacement at any point on the surface, $S_{v,max}$ is the maximum settlement right above the tunnel crown, x is the horizontal distance to the tunnel axis and i denotes the horizontal distance of the inflection point of the settlement curve to the tunnel axis. Parameters $S_{v,max}$ and i can be obtained from empirical relations. Equation 2 has been suggested for parameter i as follows:

$$i = k(Z_0 - Z) \quad (2)$$

Where Z0 is the tunnel axis burial depth, Z is the vertical distance between the ground surface to the point where the calculation of settlement is of interest and k accounts for the geotechnical parameters. Also, the settled zone volume Vs is obtained from the following expression:

$$V_s = \int_{-\infty}^{+\infty} S_v(x)dx = \sqrt{2\pi} \cdot i \cdot S_{v,\max} = 2.5\, i\, S_{v,\max} \quad (3)$$

As a result, the maximum settlement is:

$$S_{v,\max} = \frac{V_s}{2.5\, i} \quad (4)$$

In this method, it is assumed that the settled zone volume is equal to the excavation volume loss V_L which is defined as follows:

$$V_L = \frac{A_{excavation} - A_{shield}}{A_{excavation}} \quad (5)$$

$A_{excavation}$ is the cross sectional area of the excavated tunnel and A_{shield} is the cross sectional area of the tunnel after the soil shrinkage behind the shield [16].

These parameters along with the cross section of the settled area are shown in Figure 2.

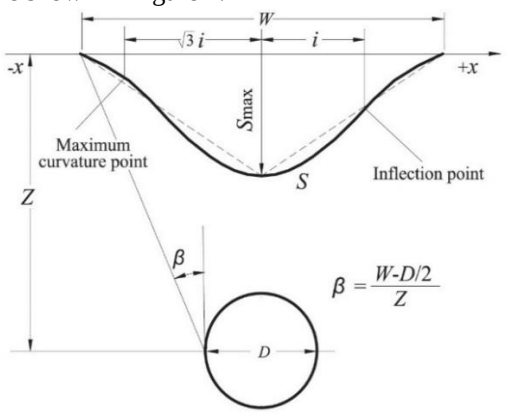

Fig. 2: Cross section of the surface settlement due to excavation

3. Numerical Modeling

This study aims to/ The aim of this study is evaluate the effect of various parameters on the risk level of surface buildings due to mechanized tunneling. by considering to parameters such as overburden depth, the building's vulnerability index, the horizontal distance to the tunnel axis, and geotechnical parameters. Baseline values were selected for all parameters. For each model, only one parameter value varied in a specified range to measure the effect of each parameter separately on the results. The baseline values and the range within which each parameter can vary, are presented in Table 1.

Table 1: Geotechnical parameters for the computational models

Number	OB (m)	E (MPa)	C (kPa)	Phi (D)
2	1.0D	80	9	34
1	**1.5D**	**80**	**9**	**34**
3	2.0D	80	9	34
4	1.5D	10	9	34
5	1.5D	45	9	34
6	**1.5D**	**80**	**9**	**34**
7	**1.5D**	**80**	**9**	**34**
8	1.5D	80	27	34
9	1.5D	80	45	34
10	1.5D	80	9	24
11	1.5D	80	9	29
12	**1.5D**	**80**	**9**	**34**

For all models, soil density is 2.03 ton/m^3, the Poisson's ratio is 0.3, and the angle of dilation and the soil tensile strength are considered to be zero.

Rows 1-3 in Table 1 represent the overburden changes, rows 4-6 represent modulus of elasticity changes, rows 7 and 8 represent the cohesion changes, and rows 10-12 represent soil angle of internal friction. The baseline values are presented in bold. The software models the cross-section perpendicular to the tunnel axis as a plane strain state. The models had different geometries due to the varying tunnel depth, surface building characteristics, and horizontal distance to the tunnel axis. The model dimensions were 80 m × 60 m. These values were chosen to prevent any effects of unrealistic boundary conditions on the model and also to decrease the computational effort. The boundary is fixed on the bottom for both x and y directions, and the roller boundary condition was applied to both sides (fixed in the x-direction).

Plastic hardening was chosen as the constitutive model as it accounts for unloading elastic modulus, leading to more realistic results for tunnel excavation problems involving unloading and stress relaxation than standard constitutive laws such as Mohr-Coulomb. In this model, contrary to Mohr-Coulomb, the unloading and reloading elastic modulus has to be defined and in this study, this parameter is set to three times the reference value of soil elastic modulus. The initial conditions of total stress were calculated considering the lateral soil pressure coefficient at rest, and they were used as the input of the software. After initial equilibrium, traffic and surface building loads were applied, and the equilibrium was reached again. The load considered for a 5-story surface building was 50 kPa applied to the upper surface of the model. A tunnel with a diameter of 9.49 m was excavated, and the walls were allowed to contract into the tunnel. The displacement of the tunnel walls was allowed to reach to a measure that the volume loss of the analytic method is obtained. In this study, volume loss was considered 0.7%.

In the following, the result of numerical modeling of the baseline model, including the computational finite differences mesh, model dimensions, tunnel excavation location, vertical displacement contour after stress relaxation until the volume loss of 0.7% and finally, the surface settlement curve are presented.

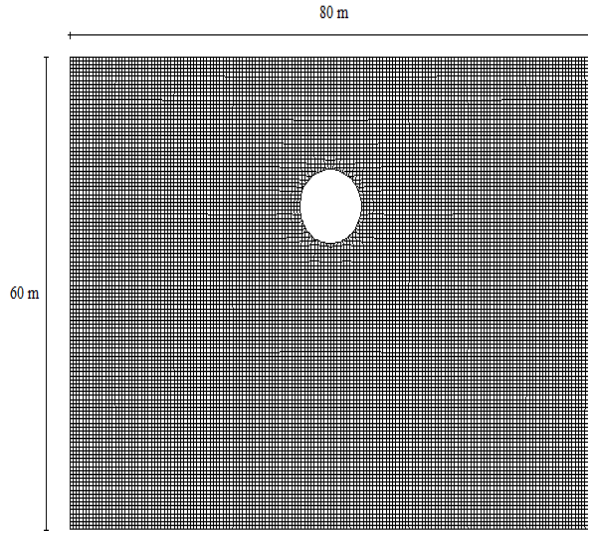

Fig. 3: Finite differences mesh, model dimensions and tunnel location for the baseline model

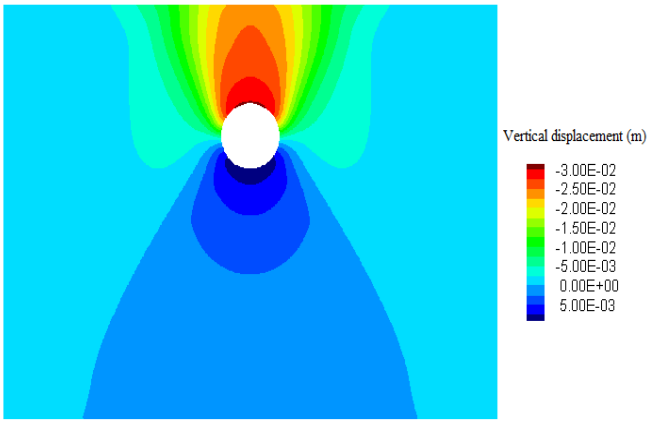

Fig. 4: Vertical displacement contour for the baseline model

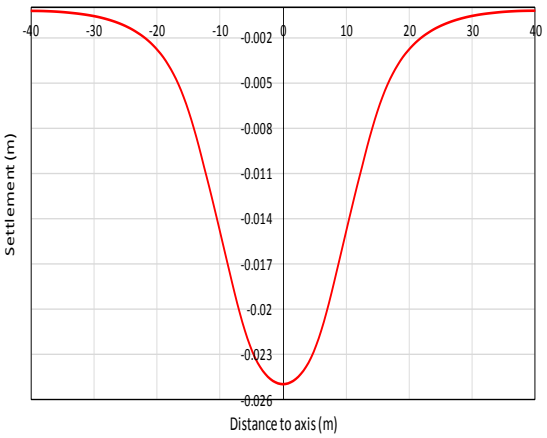

Fig. 5: Surface settlement curve for the baseline model

In order to provide a better insight into the effect of different parameters on surface settlement, figures 6 to 9 show the surface settlement for different values of overburden, modulus of elasticity, cohesion and angle of internal friction, respectively. As shown in figure 6, the lower tunnel overburden led to an increased surface settlement above the tunnel crown. However, as the horizontal distance from the tunnel axis increased, the settlement reduced significantly. Thus, the settlement curve in areas near the tunnel axis experienced a steep increase as the overburden decreased, and this may lead to a significantly high level of risk for the building due to larger strains.

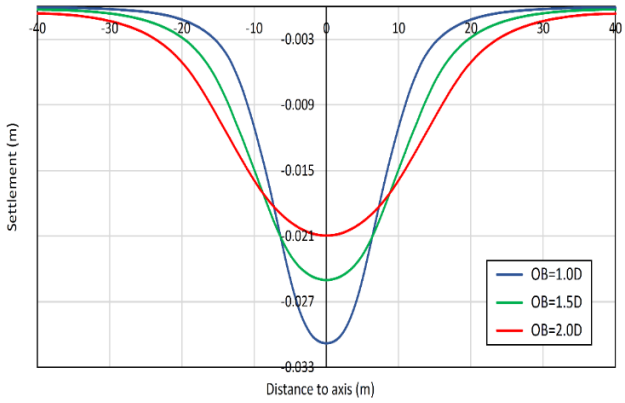

Fig. 6: Surface settlement curve for different overburdens

Figure 7 indicates that a higher modulus of elasticity resulted in higher maximum settlement (i.e., surface settlement of the ground above the tunnel axis), and the settlement decreased by getting further from the tunnel axis due to higher modulus of elasticity and thus, reduced deformation potential under tunnel excavation ,which is obvious . The higher maximum settlement compensated for lower settlement in further areas. In other words, since a 2D numerical model was developed, the volume loss was assumed to be constant (i.e., 0.7%), the maximum reduction of tunnel cross-section due to stress relaxation was equal to a volume loss of 0.7%, and volume of the settled area was approximately equal to the volume loss, the decrease volume of the settled area at further distances from the tunnel axis must be compensated for by the higher settlement of the ground above the tunnel crown.

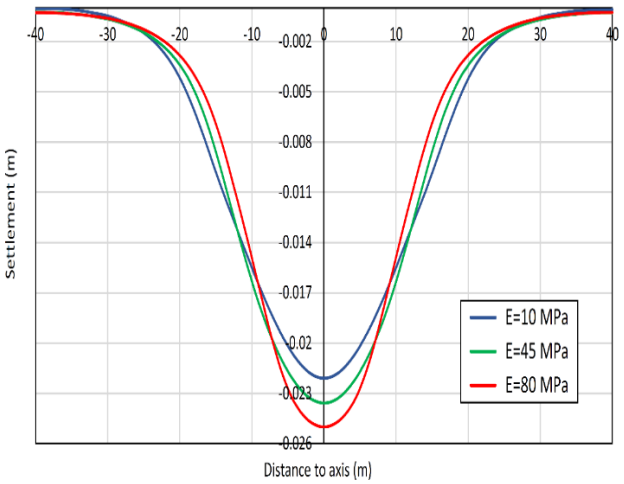

Fig. 7: Surface settlement curve for different modulus of elasticities

Figure 8 shows the surface settlement caused by excavation for different cohesions. It can be seen that as the cohesion coefficient increased, the settlement of the ground above the tunnel axis decreased, and the same settlement increased at further distances. This can be explained by the higher shear resistance and lower plastic deformations. In other words, a higher cohesion led to higher shear resistance, and consequently, lower plasticity and plastic deformations, which resulted in a lower settlement for unloaded areas above the tunnel. Since the volume of the settlement area was constant (because the volume loss was constant), the settlement of further areas is a little higher for larger cohesions.

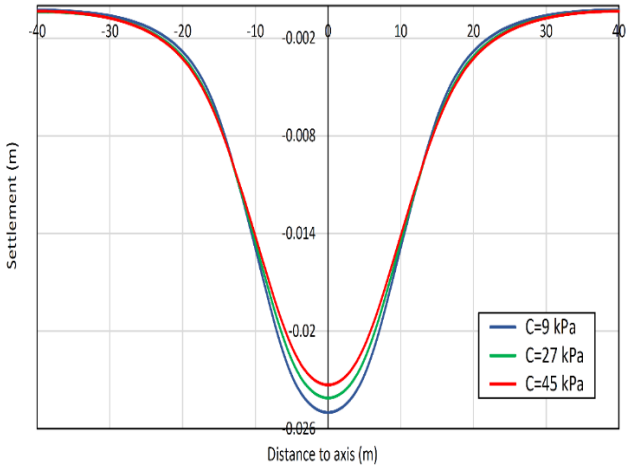

Fig. 8: Surface settlement curve for different Cohesions

As Figure 9 suggests, a larger angle of internal friction led to higher maximum settlement and lower settlement of further areas. It should be noted that excavation resulted in the unloading of areas above the tunnel crown so that the normal stresses decreased in those areas, and thus, the shear

resistance caused by friction and interlocking of particles was relatively reduced. However, the loss of shear resistance due to decreased normal stress of the ground above the tunnel crown led to plastic deformation and settlement. On the other hand, a larger angle of internal friction resulted in increased shear resistance of further areas, and thus, lower plastic deformations and settlement in those areas. Hence, the increased settlement of the ground above the tunnel crown compensated for the volume loss at the settled region, and settled volume became almost equal to the volume loss.

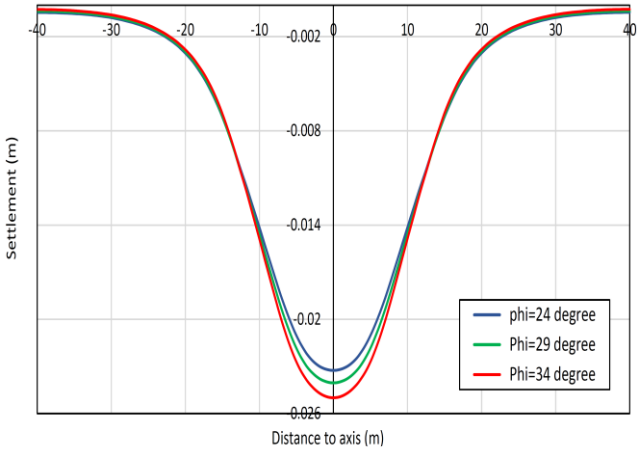

Fig. 9: Surface settlement curve for different friction angles

4. Determination of Building Risk Level

It is necessary to derive the expression for the surface settlement curve to calculate the control parameters of building settlement due to tunnel excavation-induced surface deformation. Hence, the surface settlement curve resulting from the numerical method was chosen, considering the higher accuracy of numerical methods [16].

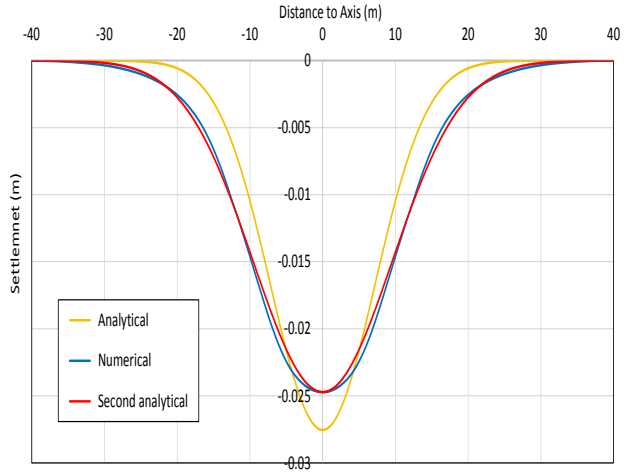

Fig. 10: Surface settlement curve for analytic, Numerical and secondary analysis for the baseline model

The parameters of Peck's equation were modified so that the analytic and numerical settlement curves would coincide. Since the volume loss was constant for both methods, parameters k and C (usually equal to 2.5) were only adjusted. The k value in Peck's analytic equation was estimated at 0.45, considering the soil type in the area. Then, the settlement curve of preliminary analysis (i.e., analytic solution with k = 0.45 and C=2.5), numerical solution, and the secondary analysis (i.e., the modified settlement expression based on numerical results) are presented in Figure 10 for the baseline model.

The C and k values obtained by fitting the analytical settlement curve to the numerical results are listed in Table 2.

Table 2: Analytical and Numerical values of *C* and *k*

Model Number	K		C	
	Analytical	Numerical	Analytical	Numerical
1	0.45	0.60	2.5	2.10
2	0.45	0.63	2.5	2.28
3	0.45	0.58	2.5	2.04
4	0.45	0.71	2.5	1.98
5	0.45	0.69	2.5	1.96
6	0.45	0.60	2.5	2.10
7	0.45	0.60	2.5	2.10
8	0.45	0.60	2.5	2.12
9	0.45	0.61	2.5	2.14
10	0.45	0.61	2.5	2.17
11	0.45	0.62	2.5	2.19
12	0.45	0.60	2.5	2.10

In order to determine the risk level for each case of Table 1, the control parameters of building settlement should be calculated for different vulnerabilities and (horizontal) distances. The building vulnerability can be obtained during Building Condition Survey (known as BCS). In this procedure, each individual surface building near the tunnel is evaluated and a vulnerability index from 0 to 10 is assigned to the building. The vulnerability index of 0-2 denotes a negligible vulnerability, while an index between 8 and 10 denotes high vulnerability. The control parameters needed for the risk assessment are the maximum vertical displacement S_{max}, maximum angular distortion β_{max} and the maximum tensile strain ε. The detailed process of calculating these control parameters are given in reference [5] and has been avoided for brevity. The interested readers can refer to the reference [5] for more details. As discussed before, the studied building (with concrete or steel frames) is a 10 m-wide, 15-m high structure with columns distance of 5 m and a 3 m-deep foundation (the bottom of the foundation was 3 m below the ground surface). Control parameters of the building settlement were calculated for all cases, leading to the determination of the level of risk for the building. The risk level is a number between 1 and 5 that specifies the level for potential risk on surface buildings in order to optimize the approaches for mitigating these risks. Knowing the vulnerability index of surface buildings and some guidelines for determining the limitations of control

parameters, the risk level (risk category or category of damage) can be obtained. Tables 3 and 4 are the guidelines given from reference [5] known as Burland and Rankin damage classifications, respectively.

Table 3: Burland damage classifications [5]

Category of damage	Vulnerability index I_v of the building									
	Negligible		Low		Slight		Medium		High	
	$0 < I_v < 20$		$20 < I_v < 40$		$40 < I_v < 60$		$60 < I_v < 80$		$80 < I_v < 100$	
	Reduction factor F_R									
	$F_R = 1.0$		$F_R = 1.25$		$F_R = 1.50$		$F_R = 1.75$		$F_R = 2.0$	
	Control parameter									
	ε_{lim} [%]		ε_{lim} [%]		ε_{lim} [%]		ε_{lim} [%]		ε_{lim} [%]	
	min.	max.	min.	max.	min.	max.	min.	max.	min.	max.
0	0,000	0,050	0,000	0,040	0,000	0,033	0,000	0,029	0,000	0,025
1	0,050	0,075	0,040	0,060	0,033	0,050	0,029	0,043	0,025	0,038
2	0,075	0,150	0,060	0,120	0,050	0,100	0,043	0,860	0,038	0,075
3	0,150	0,300	0,120	0,240	0,100	0,200	0,860	0,171	0,075	0,150
4 to 5	>0,300		>0,240		>0,200		>0,171		>0,150	

Table 4: Rankin damage classifications [5]

Category of damage	Vulnerability index I_v of the building									
	Negligible		Low		Slight		Medium		High	
	$0 < I_v < 20$		$20 < I_v < 40$		$40 < I_v < 60$		$60 < I_v < 80$		$80 < I_v < 100$	
	Reduction factor F_R									
	$F_R = 1.0$		$F_R = 1.25$		$F_R = 1.50$		$F_R = 1.75$		$F_R = 2.0$	
	Control parameter									
	S_{max} [mm]	β_{max}	S_{max} [mm]	β_{max}	S_{max} [mm]	β_{max}	S_{max} [mm]	β_{max}	S_{max} [mm]	β_{max}
1	<10	<1/500	<8	<1/625	<6,7	<1/750	<5,7	<1/875	<5	<1/1000
2	10–50	1/500–1/200	8–40	1/625–1/250	6,7–33	1/750–1/300	5,7–28,5	1/875–1/350	5–25	1/1000–1/400
3	50–75	1/200–1/50	40–60	1/250–1/63	33–50	1/300–1/75	28,5–43	1/350–1/88	25–37,5	1/400–1/100
4	>75	>1/50	>60	>1/63	>50	>1/75	>43	>1/88	>37,5	>1/100

5. Results and Discussion

In this section, for each case of Table 1, the risk level of the studied building was evaluated for different vulnerabilities and building-to-tunnel axis horizontal distances. The results are presented in subsequent figures. Dash lines represent the inflection point of the deformation curve where the concavity of the settlement curve changes.

Figures 11 to 13 show the variation of the risk level of the building with building-to-tunnel axis horizontal distance for different overburdens (OB) of 1.0D, 1.5D and 2.0D, where D denotes the tunnel diameter. It can be seen that for short building-to-tunnel axis horizontal distances, lower overburdens led to higher risk levels. However, for long building-to-tunnel axis horizontal distances, higher overburdens resulted in higher risk levels because the ground settlement curve is steeper at short building-to-tunnel axis horizontal distances for low overburdens and thus, a larger strain is imposed on the building. For high overburdens, a higher degree of settlement occurs for long building-to-tunnel axis horizontal distances, and the ground settlement curve is steeper, imposing a larger strain on the building. Furthermore, it can be seen that a higher vulnerability index resulted in a higher level of risk for the building.

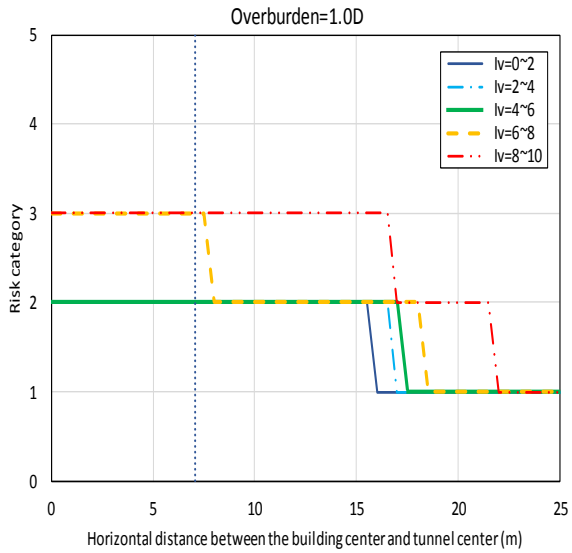

Fig. 11: Risk category for OB=1.0D and different vulnerabilities

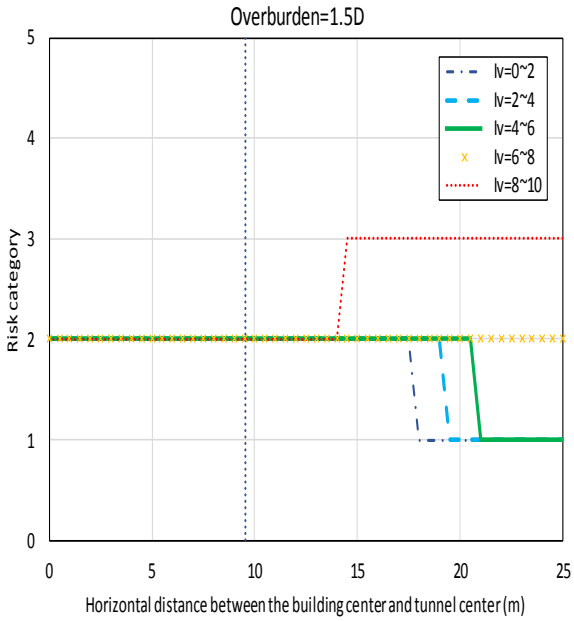

Fig. 12: Risk category for OB=1.5D and different vulnerabilities

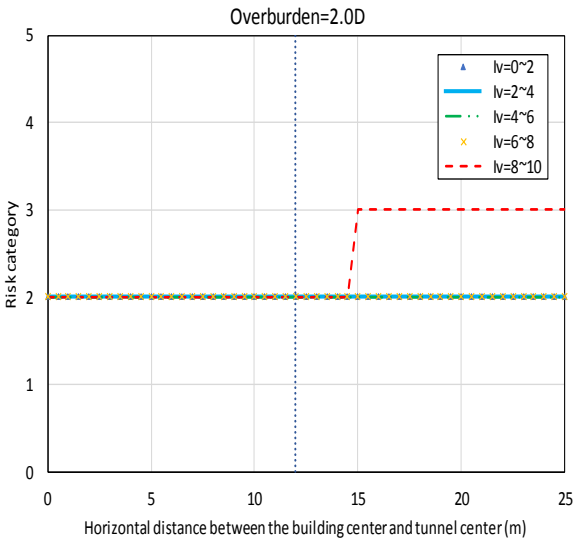

Fig. 13: Risk category for OB=2.0D and different vulnerabilities

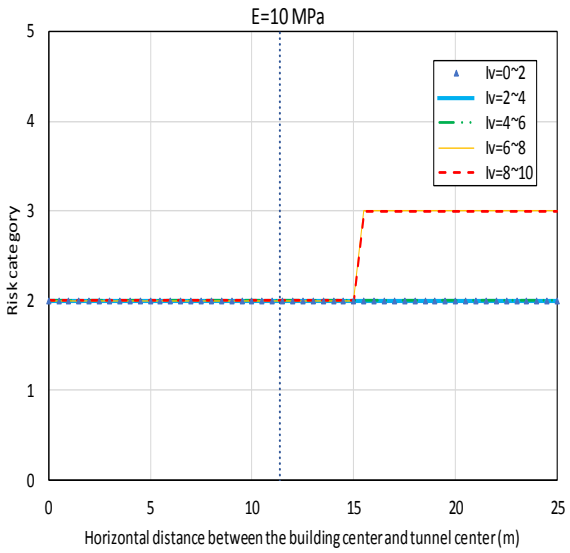

Fig. 14: Risk category for E=10 MPa and different vulnerabilities

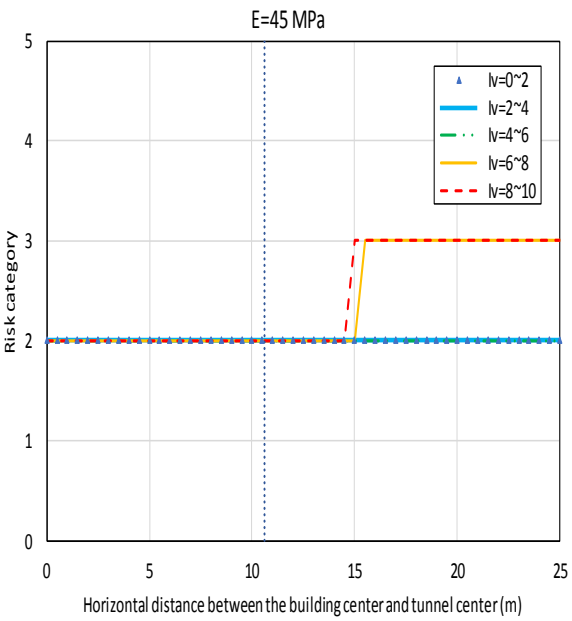

Fig. 15: Risk category for E=45 MPa and different vulnerabilities

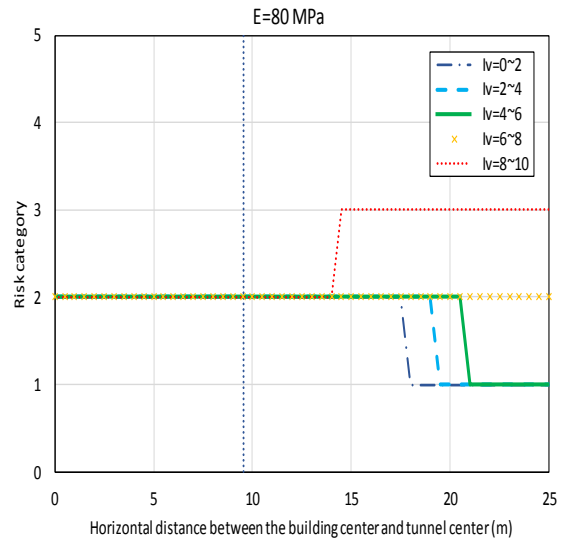

Fig. 16: Risk category for E=80 MPa and different vulnerabilities

Figures 14 to 16 show that by getting further from the tunnel axis, a higher level of risk for a small modulus of elasticity is obtained. In other words, as the modulus of elasticity decreases, buildings at further distances experience a higher risk level. If the building center is located near the inflection point of the deformation curve, the level of risk for all vulnerability indices and all cases would be below 3 due to the small strains experienced by the building.

Cohesion variations did not significantly affect the settlement curve. However, a little reduction was observed for the maximum ground settlement as the cohesion increased. Therefore, cohesion variations had no major effect on the level of risk for the building. This can be attributed to the lack of plastic deformations and, thus, the ineffectiveness of shear resistance parameters such as cohesion.

By increasing the angle of internal friction, the settlement of areas near to and far from the tunnel axis experienced a small increase and reduction, respectively. Therefore, variation of this parameter did not significantly impact the level of risk due to similar reasons as for cohesion.

6. Conclusion

The discussion above about the influencing parameters of settlement can be concluded as follows. Changing shear strength parameters of the soil, such as cohesion and angle of internal friction, affects the surface settlement curve and building risk level. However, the effect is not significant for the surface settlement because mechanized tunnel excavation is a controlled process in which soil deformations are limited. Hence, plasticity and plastic deformations play an insignificant role in settlements due to mechanized tunnel excavation. Specifically, setting a constant value for volume loss in the numerical model prohibits soil deformations higher than the specified value. If we neglectfully consider overburden (i.e., the depth of tunnel crown) as one of the geotechnical parameters, it would play a major role in the shape and magnitude of the surface settlement curve and significantly affects the risk level. It can be concluded that the modulus of elasticity was the most effective parameter for the building's risk level among the studied parameters. For a small modulus of elasticity, buildings at a further distance from the tunnel axis were exposed to a higher level of risk. Therefore, improving the soil as a control strategy is necessary, considering the soil stiffness and the building-to-tunnel axis distance.

References

[1] Atkinson, H., and Potts, D. (1977). Settlement above Shallow Tunnels in Soft Ground. Journal of Geotechnical Engineering, ASCE. 103(4): 307-325.

[2] Mair, R.J. (1998). Geotechnical Aspects of Design Criteria for Bored Tunneling in Soft Ground," Proceeding of Tunnels and Metropolises, Sao Paulo, Brazil, pp 183-199.

[3] Mahmutoglu, Y. (2010) Surface subsidence induced by twin subway tunneling in soft ground conditions in Istanbul. Bull Eng Geol Environ.

[4] Park, K.H. (2004). Elastic solution for tunneling-induced ground movements in clays. International Journal of Geomechanics, ASCE. 4(4): 310-318.

[5] Guglielmetti, V., Grasso, P., Mahtab, A., & Xu, S. (Eds.). (2008). Mechanized Tunneling in Urban Areas: Design Methodology and Construction Control (1st ed.). CRC Press.

[6] Gunn, M.J. (1993). The prediction of surface settlement profiles due to tunneling. Proceeding of the Worth Memorial Symposium, Predictive Soil Mechanics. London: Thomas Telford. 304-316.

[7] Mirhabibi, A. and Soroush, A. (2012). Effects of surface buildings on twin tunneling-induced ground settlements, Tunneling and Underground Space Technology, Vol. 29, pp 40-51.

[8] Attewell, P.B., Yeates, J., and Selby. A.R. (1986). Soil Movements Induced by Tunneling and their Effects on Pipelines and Structures. New York, Blackie.

[9] Bjerrum, L. (1963). Allowable settlement of structures. Proceedings of the European Conference on Soil Mechanics and Foundation Engineering. Wiesbaden. 2: 135-137.

[10] Hesami, S., Ahmadi, S., Hasanzadeh, A. (2013). eqGround Surface Settlement Prediction in Urban Areas due to Tunnel Excavation. Electronic journal of geotechnical engineering, 18.

[11] Park, K.H. (2004). Elastic solution for tunneling-induced ground movements in clays. International Journal of Geomechanics, ASCE. 4(4): 310-318.

[12] Bobet, A. (2001). Analytical Solutions for Shallow Tunnels in Saturated Ground. Journal of Engineering Mechanics, ASCE. 127(12): 1258-1266.

[13] Burd, H.J., Houlsby, G.T., Augarde, C.E. and Liu, G. (2000). Modelling the effects on masonry buildings of tunneling-induced settlement. Proceedings of the Institution of Civil Engineers, Geotechnical Engineering. 143(1): 17-29.

[14] Chou, W. I., and Bobet, A. (2002). Prediction of Ground Deformations in Shallow Tunnels in Clay. Tunneling and Underground Space Technology. 17: 3-19

[15] Burland, J.B., Broms, B.B., and de Mello, V.F.B. (1977). Behavior of foundations and structures. State of the Art Report. Proceeding of 9th International Conference on Soil Mechanics and Foundation Engineering. Tokyo, Japan, 495-546.

[16] Peck, R.B.: Deep Excavations and Tunneling in Soft Ground. Proc.: 7th International Conf. Soil Mechanics and Foundation Engineering, Mexico, State-of-the-art volume, State-of-the art Report, 1969, pp.225–290

[17] Burland, J.B., Wroth, C.P. (1974) Settlement of Buildings and Associated Damage. Settlement of Structures, Cambridge Pentech Press, London, Cambridge. pp. 611-654

[18] Burland, J.B. (1997). Assessment of risk of damage to buildings due to tunneling and excavation. Earthquake Geotechnical Engineering. Roterdam: Belkema. 1189-1201.

[19] Darabi, A., Ahangari, K., Noorzad, A., and Arab, A. (2012). Subsidence estimation utilizing various approaches – A case study: Tehran No. 3 subway line. Tunneling and Underground Space Technology. 31: 117–127.

[20] Chakeri, H., Ozcelik, Y., Unver, B. (2013). Effects of important factors on surface settlement prediction for metro tunnel excavated by EPB, Tunneling and Underground Space technology, Vol.36, pp 14-23.